

This discussion paper is/has been under review for the journal Earth System Dynamics (ESD). Please refer to the corresponding final paper in ESD if available.

# Spectral solar irradiance and its entropic effect on Earth's climate

W. Wu<sup>1</sup>, Y. Liu<sup>1</sup>, and G. Wen<sup>2,3</sup>

<sup>1</sup>Atmospheric Sciences Division, Brookhaven National Laboratory, Upton, NY 11973, USA

<sup>2</sup>NASA Goddard Space Flight Center, Greenbelt, Maryland, USA

<sup>3</sup>Goddard Earth Sciences and Technology Center, University of Maryland, Baltimore, Maryland, USA

Received: 14 January 2011 – Accepted: 18 January 2011 – Published: 25 January 2011

Correspondence to: W. Wu (wwu@bnl.gov)

Published by Copernicus Publications on behalf of the European Geosciences Union.

ESDD

2, 45–70, 2011

## Spectral solar irradiance and its entropic effect

W. Wu et al.

Title Page

Abstract

Introduction

Conclusions

References

Tables

Figures

◀

▶

◀

▶

Back

Close

Full Screen / Esc

Printer-friendly Version

Interactive Discussion



## Abstract

The high-resolution measurements of the spectral solar irradiance at the top of the Earth's atmosphere by the Solar Radiation and Climate Experiment (SORCE) satellite suggest significant deviation of solar radiation from the commonly assumed blackbody radiation. Here, we use these spectral irradiance measurements to estimate the Earth's incident solar radiation entropy flux, and examine the importance of a proper estimation approach. The Earth's incident solar radiation entropy flux estimated by directly applying the observed spectral solar irradiance into the most accurate Planck expression is compared with that estimated with a conventional approach that uses the Sun's brightness temperature under the assumption of a blackbody Sun. The globally averaged non-blackbody incident solar radiation entropy flux at the top of the Earth's atmosphere equals  $0.31 \text{ W m}^{-2} \text{ K}^{-1}$ . This value is about 4 times larger than that estimated from the conventional blackbody approach, with the difference comparable to the typical value of the entropy production rate associated with atmospheric latent heat process. Further analysis reveals that the decrease of spectral solar radiation entropy flux with radiation traveling distance, unlike the decrease of spectral solar radiation energy flux with radiation traveling distance, is wavelength dependent, and that the difference between the two estimates can be attributed to the fact that the conventional approach ignores the influence of radiation traveling distance on the spectral solar radiation entropy flux. Moreover, sensitivity study further shows that the distribution of top-of-atmosphere spectral solar irradiance could significantly impact the magnitude of the estimated Earth's incident solar radiation entropy flux. These results together suggest that the spectral distribution of incident solar radiation is critical for determining the Earth's incident solar radiation entropy flux, and thus the Earth's climate.

## Spectral solar irradiance and its entropic effect

W. Wu et al.

Title Page

Abstract

Introduction

Conclusions

References

Tables

Figures



Back

Close

Full Screen / Esc

Printer-friendly Version

Interactive Discussion



## 1 Introduction

Modern satellite observations have demonstrated that although the total solar irradiance (TSI) at the top of the Earth's atmosphere (TOA) varies little (only about 0.1%), the Sun is a highly variable star with a substantial variation of TOA spectral solar irradiance (SSI) (Harder et al., 2010). Because solar radiation is the primary driving force for all the activities within the Earth's climate system and radiation at different wavelengths reaches and warms different atmospheric layers, this finding raises some important questions critical to studying the Earth's climate system: What is the consequence of the changing TOA SSI to the Earth's climate system? Could this finding change our view of greenhouse-gas induced global climate change?

Based on the daily observations of the solar spectrum between 200 nm and 2400 nm from the Spectral Irradiance Monitor (SIM) instrument on the Solar Radiation and Climate Experiment (SORCE) satellite, Harder et al. (2010) found that the primary contributors to TSI (i.e., irradiance at ultraviolet, visible, and near infrared wavelengths) exhibit significantly different variability with time. The irradiance at ultraviolet (200 nm to 400 nm) wavelengths shows a significant decline in this period while the irradiance at visible (400 nm to 691 nm) or near infrared (972 nm to 2423 nm) wavelengths shows a large increase and the irradiance at near infrared (691 nm to 972 nm) wavelengths shows a small decrease (see Fig. 3 in Harder et al., 2010). It has been known that radiation at ultraviolet wavelengths mainly heats stratosphere and is critical to producing stratospheric ozone, and radiation at visible and near infrared wavelengths mainly heats troposphere as well as the Earth's surface. Thus, the significantly different variability of the primary contributors to TSI is intuitively expected to have a large impact on the vertical profiles of atmospheric ozone and temperature as well as the Earth's surface temperature.

A series of recent papers has investigated the Earth's climate responses to the TOA SSI variability as reported by Harder et al. (2010), suggesting that the impacts of the TOA SSI variability on the Earth's climate system could be significantly different from

## Spectral solar irradiance and its entropic effect

W. Wu et al.

Title Page

Abstract

Introduction

Conclusions

References

Tables

Figures



Back

Close

Full Screen / Esc

Printer-friendly Version

Interactive Discussion



**Spectral solar irradiance and its entropic effect**

W. Wu et al.

Title Page

Abstract

Introduction

Conclusions

References

Tables

Figures



Back

Close

Full Screen / Esc

Printer-friendly Version

Interactive Discussion



our current understanding, especially on the vertical profiles of atmospheric ozone and temperature (e.g., Cahanlan et al. 2010; Haigh et al., 2010). For example, Cahanlan et al. (2010) used the findings by Harder et al. (2010) to construct two 11-year sinusoidal scenarios of TOA SSI forcing with the same TSI. One has out-of-phase SSI variability as in the SIM-based observations and the other has in-phase SSI variability as the reconstructed solar radiation from a widely used solar radiation reconstruction model by Lean (2000). Then, they used the two scenarios of TOA SSI forcing to drive a radiative-convective model and a global climate model (i.e., NASA Goddard Institute for Space Studies modelE) to investigate the difference of the Earth's climate responses. They found that the two scenarios lead to significantly different climate responses, especially in upper stratosphere where temperature response to the out-of-phase scenario shows 5 times larger than that to the in-phase scenario. Additionally, Haigh et al. (2010) employed a radiative photochemical model to investigate the impact of the SIM-based out-of-phase TOA SSI variability on stratosphere by comparing with the Lean-model reconstructed in-phase TOA SSI variability. They found that the SIM-based out-of-phase TOA SSI variability could lead to a significant decline in stratospheric ozone below an altitude of 45 km from 2004 to 2007 and an increase above this altitude. Besides, they also found that according to the SIM-based TOA SSI observations the tropopause SSI has an increase over the declining phase of solar cycle 23 (i.e., out-of-phase with declining solar activity from 2004 to 2007), which is opposite to our previous understanding. Furthermore, Gray et al. (2010) reviewed current understanding of the influence of solar variability on the Earth's climate system from solar variability, solar-terrestrial interactions and the mechanisms determining the response of the Earth's climate system. They emphasized that if the out-of-phase TOA SSI variability in the SIM-based observations is real, responses in both stratospheric ozone and temperature are expected to be much different from current expectations as indicated by Haigh et al. (2010) and thus need to be reassessed. They suggested a need for further observations and research for improving our understanding of solar forcing mechanisms and their impacts on the Earth's climate system, including understanding

the SIM-based out-of-phase TOA SSI variability and assessing their influence on the Earth's climate system.

Here, we are motivated to investigate entropic impact of the SIM-based out-of-phase TOA SSI variability on the Earth's climate system. Entropy, as a fundamental thermodynamic quantity additional to temperature and energy, has been shown critical for studying the Earth's climate system (e.g., Pujol and Fort, 2002; Ozawa et al., 2001; Paltridge et al., 2007; Pauluis et al. 2002a, b; Wang et al., 2008; Lucarini et al. 2010; Jupp and Cox, 2010; Lorenz, 2010; Wu and Liu, 2010b). A broad range of entropy applications on the Earth's biosphere-atmosphere system including aspects such as atmospheric circulation, role of clouds, hydrology, ecosystem exchange of energy and mass can be found in a special issue published in Philosophical Transactions of the Royal Society B (Kleidon et al., 2010). The radiation exchange between the Earth's climate system and its surrounding space provides us not only the thermodynamic constraint of energy conservation dictated by the first law of thermodynamics but also the thermodynamic constraint of the overall entropy increase of the Earth's climate system associated with the second law of thermodynamics (e.g., Wu and Liu, 2010a). It is anticipated that integration of this entropy-related thermodynamic constraint into current global climate models will improve our understanding of the Earth's climate and climate change.

A proper approach to accurately calculating the overall entropy increase of the Earth's climate system is the key to investigating the entropic properties of the Earth's climate system. Calculation of the Earth's overall entropy change in turn requires knowledge of radiation entropy from the Earth's incident solar radiation (incident solar radiation entropy hereafter), radiation entropy from the Earth's reflected solar radiation, and radiation entropy from the Earth's emitted terrestrial radiation. The reflected solar and emitted terrestrial radiation entropies and the approaches for estimating them have been studied in previous papers (e.g., Stephens and O'Brien, 1993; Wu and Liu, 2010a). However, the incident solar radiation entropy has rarely been investigated, especially from the perspective of incident spectral solar irradiance.

**Spectral solar irradiance and its entropic effect**

W. Wu et al.

Title Page

Abstract

Introduction

Conclusions

References

Tables

Figures



Back

Close

Full Screen / Esc

Printer-friendly Version

Interactive Discussion



## Spectral solar irradiance and its entropic effect

W. Wu et al.

Title Page

Abstract

Introduction

Conclusions

References

Tables

Figures

⏪

⏩

◀

▶

Back

Close

Full Screen / Esc

Printer-friendly Version

Interactive Discussion



This paper focuses on examining the entropic impact of the SIM-based out-of-phase TOA SSI variability on the Earth's climate system. Conventionally, the Earth's incident solar radiation entropy is estimated by using the Sun's brightness temperature under the assumption of a blackbody Sun as proposed by Stephens and O'Brien (1993).

5 However, the SIM-based TOA SSI measurements indicate that solar radiation does not follow the blackbody radiation law as commonly assumed. Here, we take advantage of the SIM-based TOA SSI observations to investigate the magnitude and spectral distribution of the Earth's incident solar radiation entropy flux, and to examine the significance of the impact of TOA SSI variability on estimation of the Earth's incident solar radiation entropy flux.

10 Section 2 briefly introduces data and methodology used in this study. Section 3 shows the spectral distribution of the Earth's incident solar radiation entropy flux estimated by using the SIM-based TOA SSI observations. The estimated Earth's incident solar radiation entropy flux from the SIM-based TOA SSI observations is further compared with a conventional estimate by using the Sun's brightness temperature under the assumption of a blackbody Sun. Section 4 investigates the potential cause of the difference between the two estimates, by analyzing the dependence of spectral solar radiation entropy flux on radiation traveling distance. Section 5 examines the sensitivity of the Earth's incident solar radiation entropy flux to TOA SSI variability. Section 6 summarizes the main results.

## 2 Data and methodology

Daily observations of TOA SSI between 200 nm and 2400 nm have been produced through the SIM instrument on SORCE satellite since February 2003. Discussions on the SORCE SIM instrument and its product of TOA SSI data can be found in Harder et al. (2005) and Rottman et al. (2005). We use the daily SIM-based TOA SSI observations from April 2004 to October 2010 for this study of investigating the magnitude and spectral distribution of the Earth's incident solar radiation entropy flux. The

corresponding daily TOA TSI observations from the Total Irradiance Monitor (TIM) instrument on SORCE satellite are also used as a constraint of the overall solar irradiance reaching the Earth's climate system.

It is well established that Planck expression given by Eq. (1) or (2) can be used to calculate the spectral radiation entropy flux from the spectral radiation energy flux for any radiation process (Wei and Liu, 2010a).

$$L_\nu = \frac{2\kappa\nu^2}{c^2} \left\{ \left( 1 + \frac{c^2 I_\nu}{2h\nu^3} \right) \ln \left( 1 + \frac{c^2 I_\nu}{2h\nu^3} \right) - \left( \frac{c^2 I_\nu}{2h\nu^3} \right) \ln \left( \frac{c^2 I_\nu}{2h\nu^3} \right) \right\} \quad (1)$$

or

$$L_\lambda = \frac{2\kappa c}{\lambda^4} \left\{ \left( 1 + \frac{\lambda^5 I_\lambda}{2hc^2} \right) \ln \left( 1 + \frac{\lambda^5 I_\lambda}{2hc^2} \right) - \left( \frac{\lambda^5 I_\lambda}{2hc^2} \right) \ln \left( \frac{\lambda^5 I_\lambda}{2hc^2} \right) \right\} \quad (2)$$

where  $I_\nu$  (or  $I_\lambda$ ) and  $L_\nu$  (or  $L_\lambda$ ) represent spectral radiation energy and entropy fluxes per unit solid angle per unit frequency (or wavelength) respectively,  $h$ ,  $c$  and  $\kappa$  are the Planck constant, speed of light in vacuum and the Boltzmann constant respectively, and  $\nu$  (or  $\lambda$ ) represents frequency (or wavelength) variable. Planck expression was originally formulated for calculating spectral radiation entropy flux of a monochromatic (blackbody) radiation beam at thermodynamic equilibrium (Planck, 1913), and has been later demonstrated to hold also for non-blackbody radiation at a non-equilibrium condition (e.g., Wu and Liu, 2010a).

The Earth's incident solar radiation entropy flux  $J$  can then be obtained by integrating the Earth's incident spectral solar radiation entropy flux over all the frequencies (or wavelengths) through a surface with a known zenith angle  $\theta$  and solid angle  $\Omega$ ,

$$J = \int_0^\infty d\nu \int_\Omega L_\nu \cos\theta d\Omega \quad (3)$$

or

$$J = \int_0^\infty d\lambda \int_\Omega L_\lambda \cos\theta d\Omega \quad (4)$$

**Spectral solar irradiance and its entropic effect**

W. Wu et al.

Title Page

Abstract

Introduction

Conclusions

References

Tables

Figures

◀

▶

◀

▶

Back

Close

Full Screen / Esc

Printer-friendly Version

Interactive Discussion





## Spectral solar irradiance and its entropic effect

W. Wu et al.

Title Page

Abstract

Introduction

Conclusions

References

Tables

Figures



Back

Close

Full Screen / Esc

Printer-friendly Version

Interactive Discussion



Figure 1 shows the mean SIM-based TOA SSI distribution (black solid line) based on the data collected from April 2004 to October 2010. As a comparison, the TOA SSI distribution (gray dashed line) corresponding to a blackbody Sun with brightness temperature 5770 K is also shown in Fig. 1. The blackbody Sun provides the TOA TSI of  $1361 \text{ W m}^{-2}$  as the mean TIM-based TOA TSI observations from April 2004 to October 2010. Similar to the findings in Harder et al. (2010, Fig. 2), Fig. 1 shows that the irradiance at ultraviolet ( $<400 \text{ nm}$ ) wavelengths in the SIM-based TOA SSI is much smaller in magnitude than that in the TOA SSI of the blackbody Sun, suggesting that the brightness temperature of solar radiation at ultraviolet wavelengths is much cooler than that of the blackbody Sun. On the contrary, the irradiance over visible ( $400 \text{ nm}$  to  $700 \text{ nm}$ ) or the near-infrared ( $1000 \text{ nm}$  to  $2400 \text{ nm}$ ) wavelengths in the SIM-based TOA SSI is larger than that in the TOA SSI of the blackbody Sun, reflecting that the brightness temperature of solar radiation at visible and the near-infrared wavelengths is hotter than that of the blackbody Sun. The irradiance at the near-infrared ( $700 \text{ nm}$  to  $1000 \text{ nm}$ ) in the SIM-based TOA SSI shows slightly relatively cooler than that in the TOA SSI of the blackbody Sun.

Substitution of the TOA SSIs as shown in Fig. 1 into Planck expression leads to the corresponding estimates of the Earth's incident solar radiation entropy flux (Fig. 2). It is evident that the estimates of the Earth's incident solar radiation entropy flux exhibit remarkably similar patterns to their corresponding SSI distributions as shown in Fig. 1. For example, the Earth's incident solar radiation entropy flux from the SIM-based TOA SSI shows relatively low entropy flux at ultraviolet ( $<400 \text{ nm}$ ) wavelengths, relatively high entropy flux at visible ( $400 \text{ nm}$  to  $700 \text{ nm}$ ) and the near infrared ( $1000 \text{ nm}$  to  $2400 \text{ nm}$ ) wavelengths, and slightly relatively low entropy flux at the near-infrared ( $700 \text{ nm}$  to  $1000 \text{ nm}$ ). The overall Earth's incident solar radiation entropy flux within  $[200 \text{ nm}, 2400 \text{ nm}]$  wavelengths is equal to  $1.13 \text{ W m}^{-2} \text{ K}^{-1}$  for the SIM-based TOA SSI, and  $1.08 \text{ W m}^{-2} \text{ K}^{-1}$  for the blackbody Sun.

If we assume that the TOA SSI outside  $[200 \text{ nm}, 2400 \text{ nm}]$  wavelengths corresponding to the SIM-based TOA SSI observations is equal to a constant fraction of the

## Spectral solar irradiance and its entropic effect

W. Wu et al.

Title Page

Abstract

Introduction

Conclusions

References

Tables

Figures

◀

▶

◀

▶

Back

Close

Full Screen / Esc

Printer-friendly Version

Interactive Discussion



blackbody Sun's TOA SSI at the same wavelengths with its overall TSI of  $1361 \text{ W m}^{-2}$ , we obtain the overall Earth's incident solar radiation entropy flux of  $1.24 \text{ W m}^{-2} \text{ K}^{-1}$  corresponding to the SIM-based TOA SSI through Planck expression. This value is surprisingly very close to the overall Earth's incident solar radiation entropy flux of  $1.23 \text{ W m}^{-2} \text{ K}^{-1}$  by applying the blackbody Sun's TOA SSI into Planck expression. Both amount to a global averaged Earth's incident solar radiation entropy flux of  $0.31 \text{ W m}^{-2} \text{ K}^{-1}$ .

On the other hand, using the same blackbody Sun's brightness temperature ( $T_{\text{Sun}} = 5770 \text{ K}$ ), and assuming the global averaged cosine of solar zenith angle  $\cos\theta_0 = 0.25$  and solar solid angle  $\Omega_0 = 6.77 \times 10^{-5} \text{ sr}$  to the planet as in Stephens and O'Brien (1993), the conventional expression (5) yields the Earth's incident solar radiation entropy flux of  $0.08 \text{ W m}^{-2} \text{ K}^{-1}$ , 4 times smaller than that by using Planck expression and the SIM-based TOA SSI (or the blackbody Sun's TOA SSI).

#### 4 Dependence of spectral solar radiation entropy flux on radiation traveling distance

Relative to the estimated Earth's incident solar radiation entropy flux from applying the SIM-based TOA SSI into Planck expression, the significantly lower entropy flux estimated from the conventional approach seems surprising at first glance. Further inspection reveals that the large difference can be attributed to the fact that the conventional approach ignores the dependence of spectral solar radiation entropy flux on radiation traveling distance from the emission source – the Sun. This section explores this issue.

Suppose that the Sun is a blackbody with brightness temperature of  $T_{\text{Sun}}$ , the spectral solar radiation energy ( $I_{\lambda}^{\text{Sun}}$ ) and entropy ( $L_{\lambda}^{\text{Sun}}$ ) fluxes at the Sun's surface can be

written as (based on Planck's radiation theory by Planck, 1913)

$$I_{\lambda}^{\text{Sun}} = \frac{2hc^2}{\lambda^5} \left\{ \frac{1}{\exp\left(\frac{hc}{\lambda k T_{\text{Sun}}}\right) - 1} \right\} \quad (6)$$

$$L_{\lambda}^{\text{Sun}} = \frac{2Kc}{\lambda^4} \left\{ \left(1 + \frac{\lambda^5 I_{\lambda}^{\text{Sun}}}{2hc^2}\right) \ln\left(1 + \frac{\lambda^5 I_{\lambda}^{\text{Sun}}}{2hc^2}\right) - \left(\frac{\lambda^5 I_{\lambda}^{\text{Sun}}}{2hc^2}\right) \ln\left(\frac{\lambda^5 I_{\lambda}^{\text{Sun}}}{2hc^2}\right) \right\} \quad (7)$$

When the solar radiation travels to a place with a distance  $r$  to the Sun, the spectral solar radiation energy flux at this place ( $I_{\lambda}^r$ ) is inversely proportional to the square of the distance  $r$ , that is,

$$I_{\lambda}^r = \frac{r_{\text{Sun}}^2}{r^2} I_{\lambda}^{\text{Sun}} \quad (8)$$

or

$$\frac{I_{\lambda}^r}{I_{\lambda}^{\text{Sun}}} = \frac{r_{\text{Sun}}^2}{r^2} \quad (9)$$

where  $r_{\text{Sun}}$  represents the Sun's radius. Equation (9) indicates that the ratio of  $I_{\lambda}^r / I_{\lambda}^{\text{Sun}}$  is a wavelength independent variable, varying only with the distance  $r$ .

Substitution of the spectral solar radiation energy flux  $I_{\lambda}^r$  into Planck expression (2), we obtain the corresponding spectral solar radiation entropy flux at this place ( $L_{\lambda}^r$ ) as

$$L_{\lambda}^r = \frac{2Kc}{\lambda^4} \left\{ \left(1 + \frac{\lambda^5 I_{\lambda}^r}{2hc^2}\right) \ln\left(1 + \frac{\lambda^5 I_{\lambda}^r}{2hc^2}\right) - \left(\frac{\lambda^5 I_{\lambda}^r}{2hc^2}\right) \ln\left(\frac{\lambda^5 I_{\lambda}^r}{2hc^2}\right) \right\}$$

$$= \frac{2Kc}{\lambda^4} \left\{ \left(1 + \frac{r_{\text{Sun}}^2}{r^2} \frac{\lambda^5 I_{\lambda}^{\text{Sun}}}{2hc^2}\right) \ln\left(1 + \frac{r_{\text{Sun}}^2}{r^2} \frac{\lambda^5 I_{\lambda}^{\text{Sun}}}{2hc^2}\right) - \left(\frac{r_{\text{Sun}}^2}{r^2} \frac{\lambda^5 I_{\lambda}^{\text{Sun}}}{2hc^2}\right) \ln\left(\frac{r_{\text{Sun}}^2}{r^2} \frac{\lambda^5 I_{\lambda}^{\text{Sun}}}{2hc^2}\right) \right\} \quad (10)$$

Based on Eqs. (7) and (10), we obtain

$$\frac{L_{\lambda}^r}{L_{\lambda}^{\text{Sun}}} = \frac{\left(1 + \frac{r_{\text{Sun}}^2}{r^2} \frac{\lambda^{5j_{\text{Sun}}}}{2hc^2}\right) \ln\left(1 + \frac{r_{\text{Sun}}^2}{r^2} \frac{\lambda^{5j_{\text{Sun}}}}{2hc^2}\right) - \left(\frac{r_{\text{Sun}}^2}{r^2} \frac{\lambda^{5j_{\text{Sun}}}}{2hc^2}\right) \ln\left(\frac{r_{\text{Sun}}^2}{r^2} \frac{\lambda^{5j_{\text{Sun}}}}{2hc^2}\right)}{\left(1 + \frac{\lambda^{5j_{\text{Sun}}}}{2hc^2}\right) \ln\left(1 + \frac{\lambda^{5j_{\text{Sun}}}}{2hc^2}\right) - \left(\frac{\lambda^{5j_{\text{Sun}}}}{2hc^2}\right) \ln\left(\frac{\lambda^{5j_{\text{Sun}}}}{2hc^2}\right)} \quad (11)$$

Equation (11) indicates that unlike the wavelength-independent ratio of the spectral solar radiation energy flux at a place  $r$  ( $I_{\lambda}^r$ ) and that at the Sun's surface ( $I_{\lambda}^{\text{Sun}}$ ) – see Eq. (9), the ratio of the spectral solar radiation entropy flux at a place  $r$  ( $L_{\lambda}^r$ ) and that at the Sun's surface ( $L_{\lambda}^{\text{Sun}}$ )  $L_{\lambda}^r/L_{\lambda}^{\text{Sun}}$  varies with both wavelength  $\lambda$  and the distance  $r$ .

Figure 3 shows the spectral solar radiation energy flux at the Sun's surface (black solid line) and that at 1 AU scaled by  $\{\max(I_{\lambda}^{\text{Sun}})/[2\max(I_{\lambda}^{1\text{-AU}})]\}$  (gray dashed line), for a blackbody Sun with brightness temperature 5770 K. Here, we use the Sun's radius of  $6.96 \times 10^8$  m and the 1-AU distance to the Sun of  $1.49598 \times 10^{11}$  m. As expected, the two curves exhibit the same spectral distributions with one's amplitude being a constant fraction of the others. Both peak at the same wavelength. In fact, the 1-AU spectral solar radiation energy flux is not a representative of a blackbody's spectral radiation energy flux as discussed in previous papers (e.g., Fig. 2 in Wu and Liu, 2010a).

Figure 4 shows the spectral solar radiation entropy flux at the Sun's surface (black solid line) and that at 1 AU scaled by  $\{\max(L_{\lambda}^{\text{Sun}})/[2\max(L_{\lambda}^{1\text{-AU}})]\}$  (gray dashed line), for the blackbody Sun with brightness temperature 5770 K as in Fig. 3. Unlike the spectral solar radiation energy fluxes at the Sun's surface and that at 1 AU which have the same spectral distributions, the spectral distributions of the two corresponding spectral solar radiation entropy fluxes are different. As can be seen from Fig. 4, the peak of the spectral solar radiation entropy flux at 1 AU slightly shifts to the right (larger wavelength) compared with that at the Sun's surface. In addition, the reduction on amplitude of spectral solar radiation entropy flux because of radiation traveling distance shown in Fig. 4 is wavelength dependent.

## Spectral solar irradiance and its entropic effect

W. Wu et al.

Title Page

Abstract

Introduction

Conclusions

References

Tables

Figures



Back

Close

Full Screen / Esc

Printer-friendly Version

Interactive Discussion



Figure 5 further illustrates this point by plotting the ratio of spectral solar radiation energy flux at the Sun's surface and that at 1 AU (i.e.,  $I_{\lambda}^{\text{Sun}} / I_{\lambda}^{1\text{-AU}}$ ) and the ratio of spectral solar radiation entropy flux at the Sun's surface and that at 1 AU (i.e.,  $L_{\lambda}^{\text{Sun}} / L_{\lambda}^{1\text{-AU}}$ ). The former presents a constant for all the wavelengths but the latter decreases quickly with the increase of wavelength.

Note that, the conventional expression (5) for estimating the Earth's incident solar radiation entropy flux ignores the dependence of spectral solar radiation entropy flux on radiation traveling distance implicitly. This neglect is probably the main reason responsible for the significant underestimation of the Earth's incident solar radiation entropy flux by the conventional approach as presented in Sect. 3.

### 5 Sensitivity of the Earth's incident solar radiation entropy flux to TOA SSI variability

To further explore the sensitivity of the Earth's incident solar radiation entropy flux to TOA SSI variability, this section uses the mean SIM-based TOA SSI distribution within [200 nm, 2400 nm] wavelengths and construct two additional TOA SSI scenarios in the corresponding wavelengths. The two constructed TOA SSI scenarios have the same overall solar irradiance within the range of wavelength from 200 nm to 2400 nm as the mean SIM-based TOA SSI. Scenario I represents the TOA SSI of a blackbody Sun. Scenario II represents the TOA SSI of a non-blackbody Sun, with the Sun's brightness temperature represented by a combination of two half-period sinusoidal curves over [200 nm, 800 nm] wavelengths and over [801 nm, 2400 nm] wavelengths. The incident spectral solar radiation entropy fluxes  $L_{\lambda}$  over the wavelength range from 200 nm to 2400 nm are examined using Planck expression for the three cases. Integration of  $L_{\lambda}$  over the wavelength range from 200 nm to 2400 nm and over a hemisphere under the assumption of isotropic incident solar radiation further leads to the overall incident solar radiation entropy flux within [200 nm, 2400 nm] wavelengths. The magnitudes

and spectral distributions of the resulting Earth's incident solar radiation entropy fluxes within [200 nm, 2400 nm] wavelengths for the three cases are then compared.

Figure 6 shows the Sun's brightness temperature as a function of wavelength within [200 nm, 2400 nm] corresponding to the mean SIM-based TOA SSI distribution (black solid line) and the two constructed TOA SSI scenarios (gray dashed or dotted lines) as described above. The distributions of their corresponding Earth's incident spectral solar radiation energy flux are shown in Fig. 7.

Figure 8 shows the Earth's incident spectral solar radiation entropy flux for the three cases. As can be seen, the Earth's incident solar radiation entropy fluxes present similar patterns to their corresponding incident solar radiation energy fluxes as shown in Fig. 7. Compared with scenario I (a blackbody Sun), the Earth's incident solar radiation entropy flux from the SIM-based TOA SSI shows relatively low entropy flux at ultraviolet (<400 nm) wavelengths, relatively high entropy flux at visible (400 nm to 700 nm) and the near infrared (1000 nm to 2400 nm) wavelengths, and slightly relatively low entropy flux at the near-infrared (700 nm to 1000 nm). On the other hand, the Earth's incident solar radiation entropy flux from scenario II (a non-blackbody Sun) in general is much lower at the wavelengths less than 800 nm and much higher at the wavelengths larger than 800 nm than those from the other two cases, except for the wavelengths less than 280 nm where the Earth's incident solar radiation entropy flux from the SIM-based TOA SSI is much lower than that from the others.

By further integrating the Earth's incident spectral solar radiation entropy flux over the wavelength range of [200 nm, 2400 nm] and over a hemisphere under the assumption of isotropic incident solar radiation, we obtain the estimates of the overall Earth's incident solar radiation entropy flux within [200 nm, 2400 nm] wavelengths for the three cases. They are  $1.13 \text{ W m}^{-2} \text{ K}^{-1}$  for the mean SIM-based TOA SSI,  $1.09 \text{ W m}^{-2} \text{ K}^{-1}$  for scenario I, and  $1.40 \text{ W m}^{-2} \text{ K}^{-1}$  for scenario II. In other words, the overall incident solar radiation entropy flux within [200 nm, 2400 nm] from the mean SIM-based TOA SSI (or scenario II) is  $0.04 \text{ W m}^{-2} \text{ K}^{-1}$  (i.e., 4%) [or  $0.31 \text{ W m}^{-2} \text{ K}^{-1}$  (i.e., 28%)] larger than that from scenario I. Notice that, the difference of  $0.31 \text{ W m}^{-2} \text{ K}^{-1}$  is more than the

## Spectral solar irradiance and its entropic effect

W. Wu et al.

Title Page

Abstract

Introduction

Conclusions

References

Tables

Figures



Back

Close

Full Screen / Esc

Printer-friendly Version

Interactive Discussion



typical value of the entropy production rate associated with the atmospheric latent heat process  $0.30 \text{ W m}^{-2} \text{ K}^{-1}$  according to Peixoto et al. (1991).

## 6 Summary

The magnitude and spectral distribution of the Earth's incident solar radiation entropy flux are examined using the TOA SSI observations from the SORCE SIM instrument. The Earth's incident solar radiation entropy flux estimated by using the SIM-based TOA SSI and Planck expression of spectral radiation entropy flux is compared with that estimated by using a conventional expression based on the Sun's brightness temperature under the assumption of a blackbody Sun. The potential cause of the large difference between the two estimates is revealed. Furthermore, sensitivity experiments are performed to investigate the significance of the impact of TOA SSI variability on estimation of the Earth's incident solar radiation entropy flux.

The Earth's incident solar radiation entropy flux estimated using the mean SIM-based TOA SSI observations and Planck expression exhibits 4 times larger in magnitude than that estimated using the conventional expression based on the Sun's brightness temperature under the assumption of a blackbody Sun. It is worth emphasizing that the difference ( $0.23 \text{ W m}^{-2} \text{ K}^{-1}$ ) between the two approaches represents about 77% of the typical entropy production rate associated with the atmospheric latent heat process (Peixoto et al., 1991). It is shown that the decrease of spectral solar radiation entropy flux with radiation traveling distance, unlike the decrease of spectral solar radiation energy flux with radiation traveling distance, is wavelength dependent. The conventional approach using a blackbody Sun's brightness temperature does not account for the effect of radiation traveling distance on spectral solar radiation entropy flux, resulting in the significant underestimation of the Earth's incident solar radiation entropy flux.

Moreover, our sensitivity experiments show that even for the same overall TOA solar irradiance, the Earth's incident solar radiation entropy flux can change significantly in both magnitude and spectral distribution with the change of TOA SSI distribution.

### Spectral solar irradiance and its entropic effect

W. Wu et al.

Title Page

Abstract

Introduction

Conclusions

References

Tables

Figures



Back

Close

Full Screen / Esc

Printer-friendly Version

Interactive Discussion



## Spectral solar irradiance and its entropic effect

W. Wu et al.

Title Page

Abstract

Introduction

Conclusions

References

Tables

Figures

◀

▶

◀

▶

Back

Close

Full Screen / Esc

Printer-friendly Version

Interactive Discussion



The difference in magnitude of the resulting Earth's incident solar radiation entropy flux between some cases could be larger than the typical value of the entropy production rate associated with the atmospheric latent heat process. These results together highlight the importance and necessity of knowing the non-blackbody TOA SSI variability in calculation of the Earth's incident solar radiation entropy flux, and hence the Earth's radiation entropy budget and climate.

It is noted that this study is just a beginning to explore the importance of spectral solar irradiance and its variation in determining the Earth's radiation entropy and climate. Much remains to be learned. For example, the relative agreement between the overall magnitudes of the Earth's incident solar radiation entropy flux by applying the mean SIM-based TOA SSI or the TOA SSI from a corresponding blackbody Sun (i.e., with the same amount of TOA TSI) into Planck expression holds only true for the cases investigated here. Large discrepancy cannot be ruled out for other cases. Also, little has been known on the potential influences of SSI variability on the entropy production by processes occurring in the Earth's climate system, such as clouds and precipitation. Research along these lines is highly recommended.

*Acknowledgements.* This work is supported by the ESM (Earth System Modeling) through the FASTER project ([www.bnl.gov/esm](http://www.bnl.gov/esm)), and ASR (Atmospheric Science Research) programs of the US Department of Energy. We are grateful to Stephen E. Schwartz at BNL for valuable discussions.

## References

- Cahalan, R. F., Wen, G. Y., Harder, J. W., and Pilewskie, P.: Temperature responses to spectral solar variability on decadal time scales, *Geophys. Res. Lett.*, 37, L07705, doi:10.1029/2009GL041898, 2010.
- Gray, L. J., Beer, J., Geller, M., Haigh, J. D., Lockwood, M., Matthes, K., Cubasch, U., Fleitmann, D., Harrison, G., Hood, L., Luterbacher, J., Meehl, G. A., Shindell, D., Van Geel, B., and White, W.: Solar influences on climate, *Rev. Geophys.*, 48, RG4001, doi:10.1029/2009RG000282, 2010.

## Spectral solar irradiance and its entropic effect

W. Wu et al.

Title Page

Abstract

Introduction

Conclusions

References

Tables

Figures

◀

▶

◀

▶

Back

Close

Full Screen / Esc

Printer-friendly Version

Interactive Discussion



Haigh, J. D., Winning, A. R., Toumi, R., and Harder, J. W.: An influence of spectral solar variations on radiative forcing of climate, *Nature*, 467, 696–699, doi:10.1038/nature09426, 2010.

Harder, J., Lawrence, G., Fontenla, J., Rottman, G., and Woods, T.: The spectral irradiance monitor: Scientific requirements, instrument design, and operation modes, *Sol. Phys.*, 230, 141–167, 2005.

Harder, J. W., Fontenla, J. M., Pilewskie, P., Richard, E. C., and Woods, T. N.: Trends in spectral solar irradiance variability in the visible and infrared, *Geophys. Res. Lett.*, 36, L07801, doi:10.1029/2008GL036797, 2009.

Jupp, T. E. and Cox, P. M.: MEP and planetary climates: insights from a two-box climate model containing atmospheric dynamics, *Phil. Trans. R. Soc. B*, 365, 1355–1365, doi:10.1098/rstb.2009.0297, 2010.

Kleidon, A., Malhi, Y., and Cox, P. M.: Maximum entropy production in environmental and ecological systems, *Philos. Trans. R. Soc. B*, 365, 1297–1302, doi:10.1098/rstb.2010.0018, 2010.

Lean, J.: Evolution of the Sun's spectral irradiance since the Maunder minimum, *Geophys. Res. Lett.*, 27, 2425–2428, 2000.

Lorenz, R.: The two-box model of climate: limitations and applications to planetary habitability and maximum entropy production studies, *Phil. Trans. R. Soc. B*, 365, 1349–1354, doi:10.1098/rstb.2009.0312, 2010.

Lucarini, V., Fraedrich, K., and Lunkeit, F.: Thermodynamics of climate change: generalized sensitivities, *Atmos. Chem. Phys.*, 10, 9729–9737, doi:10.5194/acp-10-9729-2010, 2010.

Ozawa, H., Shimokawa, S., and Sakuma, H.: Thermodynamics of fluid turbulence: A unified approach to the maximum transport properties, *Phys. Rev. E*, 64, 026303, doi:10.1103/PhysRevE.64.026303, 2001.

Pauluis, O. and Held, I. M.: Entropy budget of an atmosphere in radiative-convective equilibrium. Part I: Maximum work and frictional dissipation, *J. Atmos. Sci.*, 59, 125–139, 2002a.

Pauluis, O. and Held, I. M.: Entropy budget of an atmosphere in radiative-convective equilibrium. Part II: Latent heat transport and moist processes, *J. Atmos. Sci.*, 59, 140–149, 2002b.

Paltridge, G. W., Farquhar, G. D., and Cuntz, M.: Maximum entropy production, cloud feedback, and climate change. *Geophys. Res. Lett.*, 34, 1–6, L14708, doi:10.1029/2007GL029925, 2007.

Peixoto, J. P., Oort, A. H., De Almeida, M., and Tomé, A.: Entropy budget of the atmosphere, *J.*

## Spectral solar irradiance and its entropic effect

W. Wu et al.

Title Page

Abstract

Introduction

Conclusions

References

Tables

Figures

⏪

⏩

◀

▶

Back

Close

Full Screen / Esc

Printer-friendly Version

Interactive Discussion



Geophys. Res., 96, 10981–10988, doi:10.1029/91JD00721, 1991.

Planck, M.: The Theory of Heat Radiation, 224 pp., 1913, English translation by Morton Mau-  
sius (1914), Dover Publications, New York, 1959.

Pujol, T. and Fort, J.: States of maximum entropy production in a one-dimensional vertical  
5 model with convective adjustment, *Tellus*, 54A, 363–369, 2002.

Rottman, G., Harder, J., Fontenla, J., Woods, T. N., White, O. R., and Lawrence, G.: The  
Spectral Irradiance Monitor (SIM): Early observations, *Sol. Phys.*, 230, 205–224, 2005.

Stephens, G. L. and O'Brien, D. M.: Entropy and climate, I, ERBE observations of the entropy  
production, *Q. J. R. Meteorol. Soc.*, 119, 121–152, 1993.

10 Wang, B., Nakajima, T., and Shi, G.: Cloud and Water Vapor Feedbacks in a Vertical  
Energy-Balance Model with Maximum Entropy Production, *J. Clim.*, 21, 6689–6697, doi:  
10.1175/2008JCLI2349.1., 2008.

Wu, W. and Liu Y.: Radiation entropy flux and entropy production of the Earth system, *Rev.*  
*Geophys.*, 48, RG2003, doi:10.1029/2008RG000275, 2010a.

15 Wu, W. and Liu, Y.: A new one-dimensional radiative equilibrium model for investi-  
gating atmospheric radiation entropy flux, *Philos. Trans. R. Soc. B*, 365, 1367–1376,  
doi:10.1098/rstb.2009.0301, 2010b.

**Spectral solar irradiance and its entropic effect**

W. Wu et al.

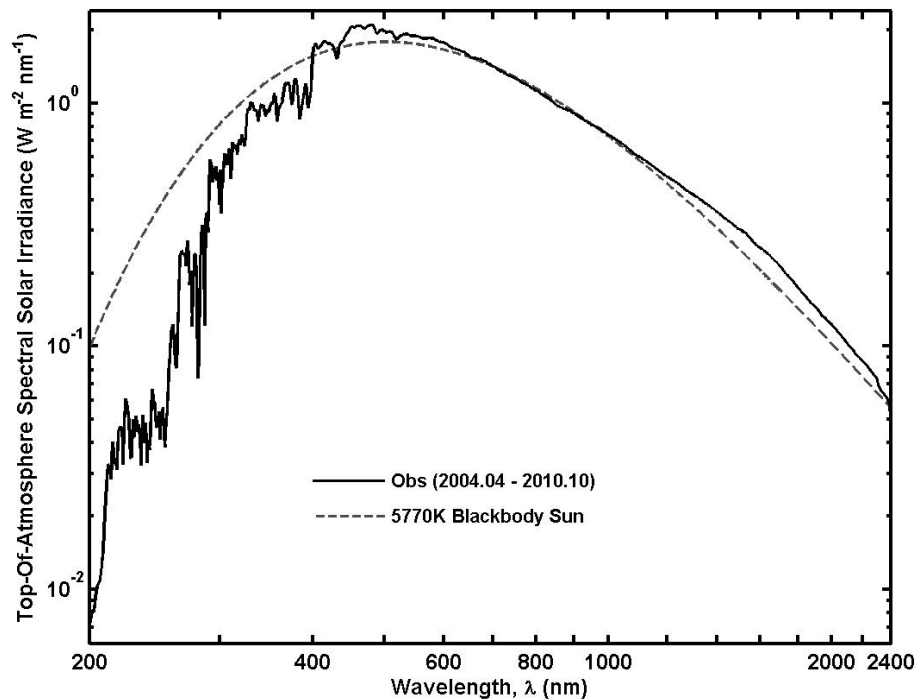


**Fig. 1.** Black solid line represents the mean SIM-based TOA SSI distribution based on the data collected from April 2004 to October 2010. Gary dashed line represents the TOA SSI distribution corresponding to a blackbody Sun with brightness temperature 5770 K.

Full Screen / Esc

Printer-friendly Version

Interactive Discussion



## Spectral solar irradiance and its entropic effect

W. Wu et al.

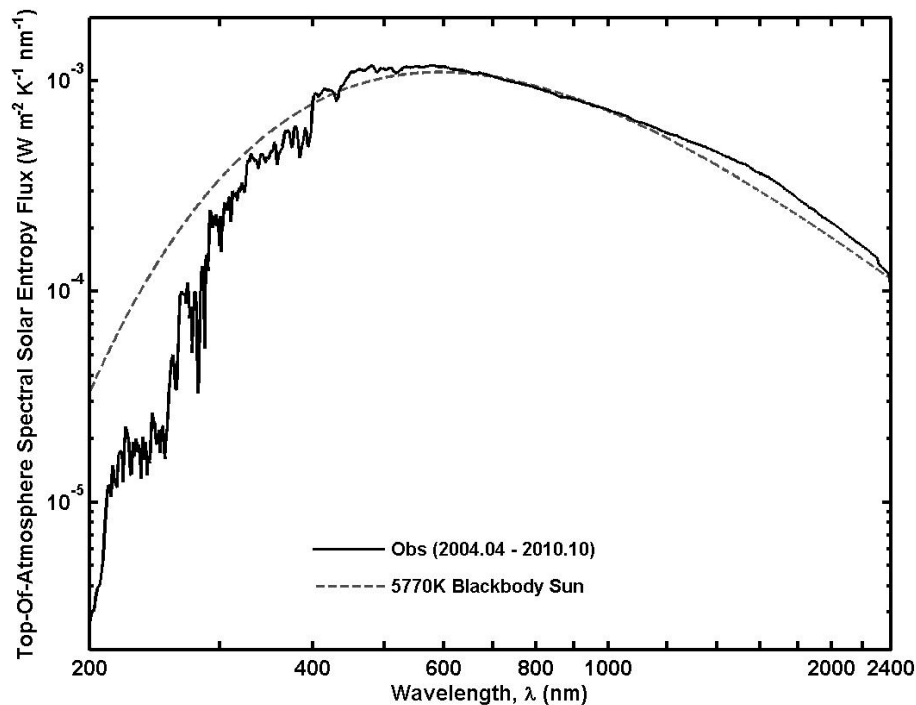


**Fig. 2.** The Earth's incident spectral solar radiation entropy flux corresponding to the TOA SSIs as shown in Fig. 1.

[Title Page](#)[Abstract](#)[Introduction](#)[Conclusions](#)[References](#)[Tables](#)[Figures](#)[◀](#)[▶](#)[◀](#)[▶](#)[Back](#)[Close](#)[Full Screen / Esc](#)[Printer-friendly Version](#)[Interactive Discussion](#)

## Spectral solar irradiance and its entropic effect

W. Wu et al.

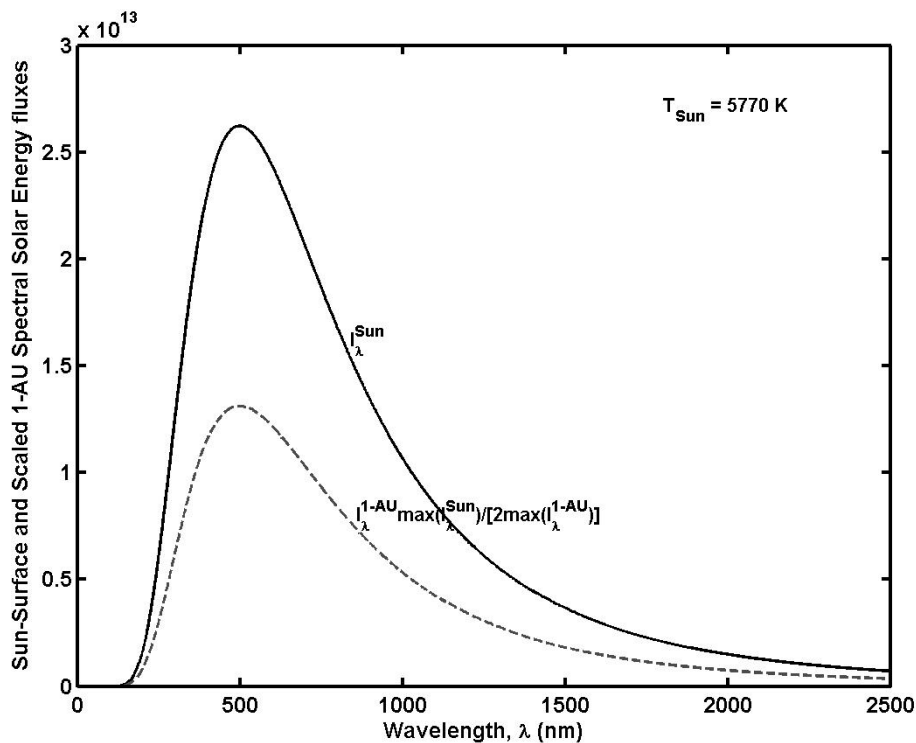


**Fig. 3.** Spectral solar radiation energy flux at the Sun's surface (black solid line) and that at 1 AU scaled by  $\{\max(I_{\lambda}^{\text{Sun}})/[2\max(I_{\lambda}^{\text{1-AU}})]\}$  (gray dashed line), for a blackbody Sun with brightness temperature 5770 K.

Title Page

Abstract

Introduction

Conclusions

References

Tables

Figures

◀

▶

◀

▶

Back

Close

Full Screen / Esc

Printer-friendly Version

Interactive Discussion



## Spectral solar irradiance and its entropic effect

W. Wu et al.

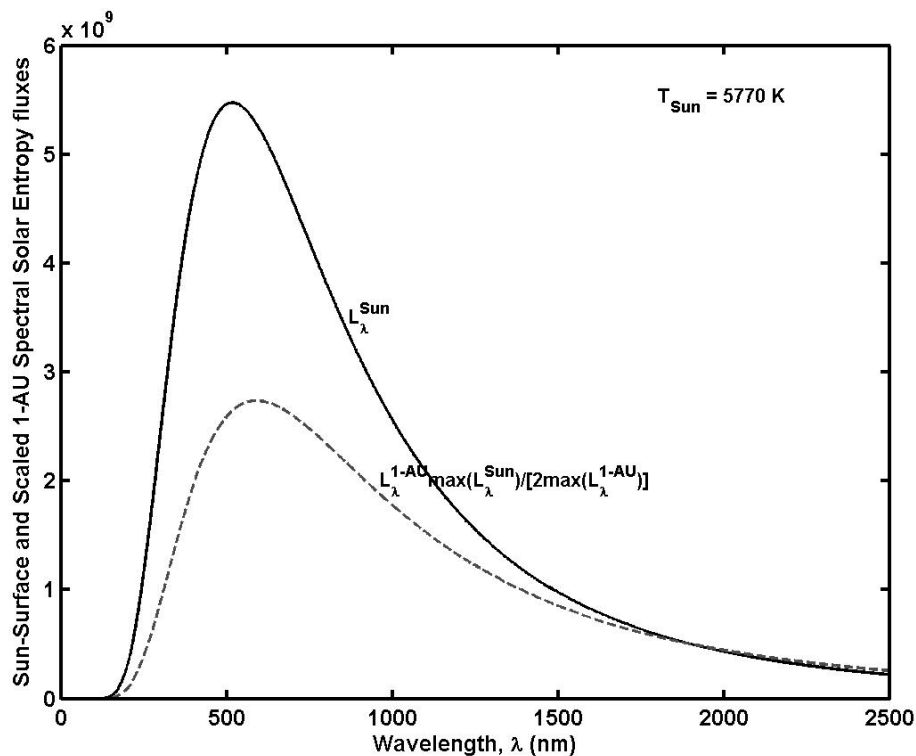


**Fig. 4.** Spectral solar radiation entropy flux at the Sun's surface (black solid line) and that at 1 AU scaled by  $\{\max(L_{\lambda}^{\text{Sun}})/[2\max(L_{\lambda}^{1\text{-AU}})]\}$  (gray dashed line), for a blackbody Sun with brightness temperature 5770 K.

Title Page

Abstract

Introduction

Conclusions

References

Tables

Figures

◀

▶

◀

▶

Back

Close

Full Screen / Esc

Printer-friendly Version

Interactive Discussion



## Spectral solar irradiance and its entropic effect

W. Wu et al.

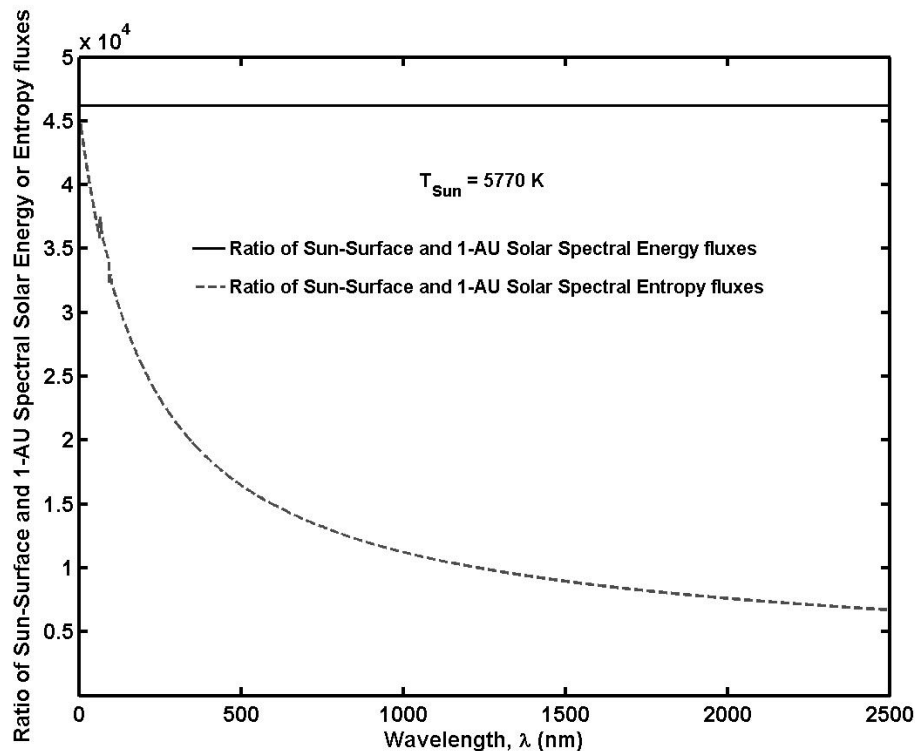


**Fig. 5.** Black solid line: the ratio of spectral solar radiation energy flux at the Sun’s surface and that at 1 AU, for a blackbody Sun with brightness temperature 5770 K. Gray dashed line: the ratio of spectral solar radiation entropy flux at the Sun’s surface and that at 1 AU for the same blackbody Sun.

Title Page

Abstract

Introduction

Conclusions

References

Tables

Figures

◀

▶

◀

▶

Back

Close

Full Screen / Esc

Printer-friendly Version

Interactive Discussion



**Spectral solar irradiance and its entropic effect**

W. Wu et al.

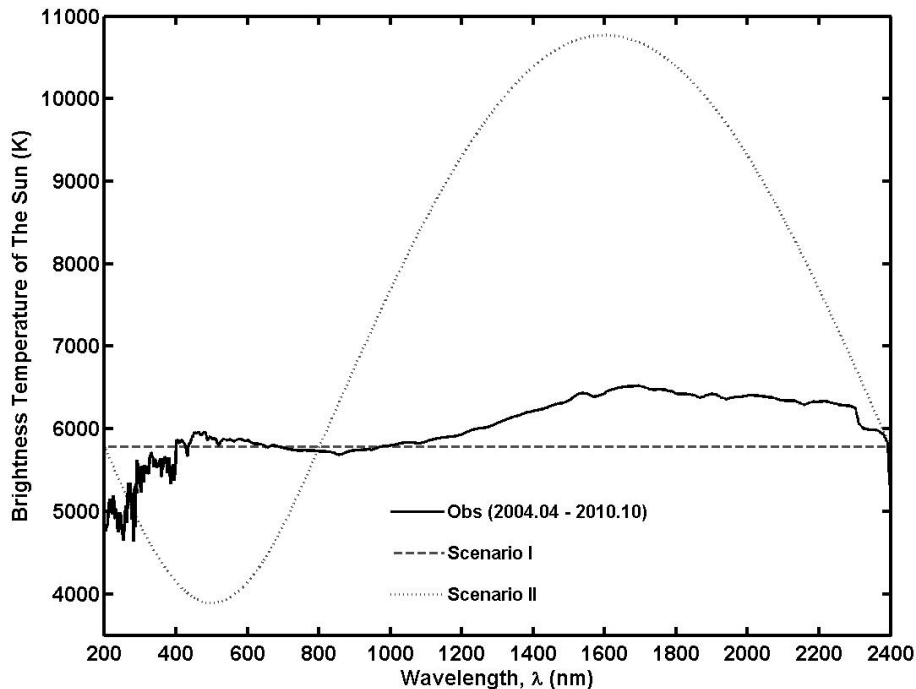


**Fig. 6.** The Sun's brightness temperature as a function of wavelength within [200 nm, 2400 nm]. Black solid line: brightness temperature corresponding to the mean SIM-based SSI from April 2004 to October 2010. Gray dashed or dotted lines: brightness temperatures corresponding to the two constructed TOA SSI scenarios with the same overall solar irradiance within the range of wavelength from 200 nm to 2400 nm as the mean SIM-based TOA SSI.

Title Page

Abstract

Introduction

Conclusions

References

Tables

Figures

◀

▶

◀

▶

Back

Close

Full Screen / Esc

Printer-friendly Version

Interactive Discussion



**Spectral solar irradiance and its entropic effect**

W. Wu et al.

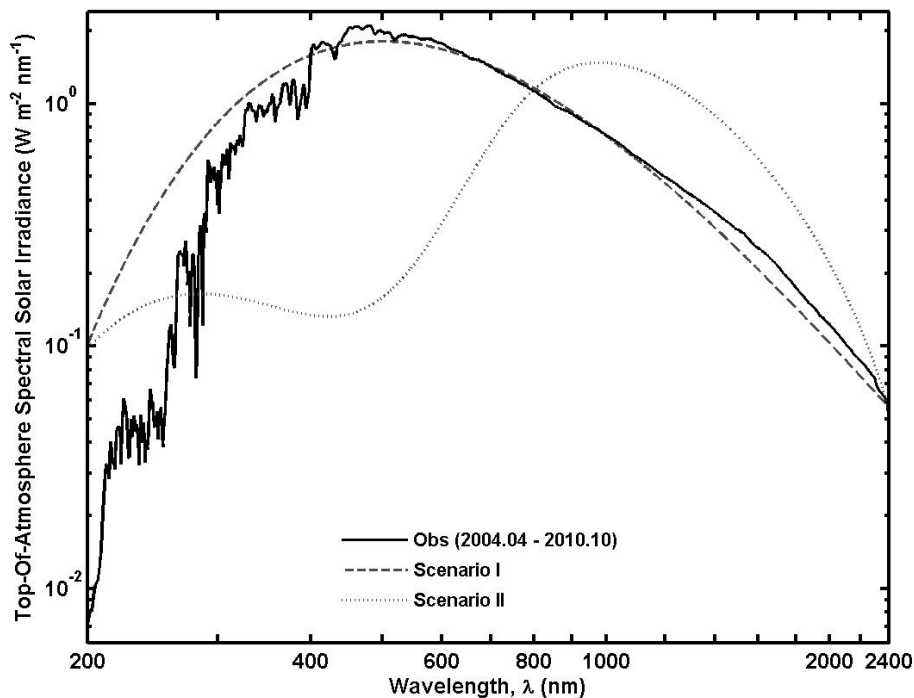


**Fig. 7.** The Earth's incident spectral solar radiation energy flux for the three cases as shown in Fig. 6.

[Title Page](#)[Abstract](#)[Introduction](#)[Conclusions](#)[References](#)[Tables](#)[Figures](#)[◀](#)[▶](#)[◀](#)[▶](#)[Back](#)[Close](#)[Full Screen / Esc](#)[Printer-friendly Version](#)[Interactive Discussion](#)

**Spectral solar irradiance and its entropic effect**

W. Wu et al.

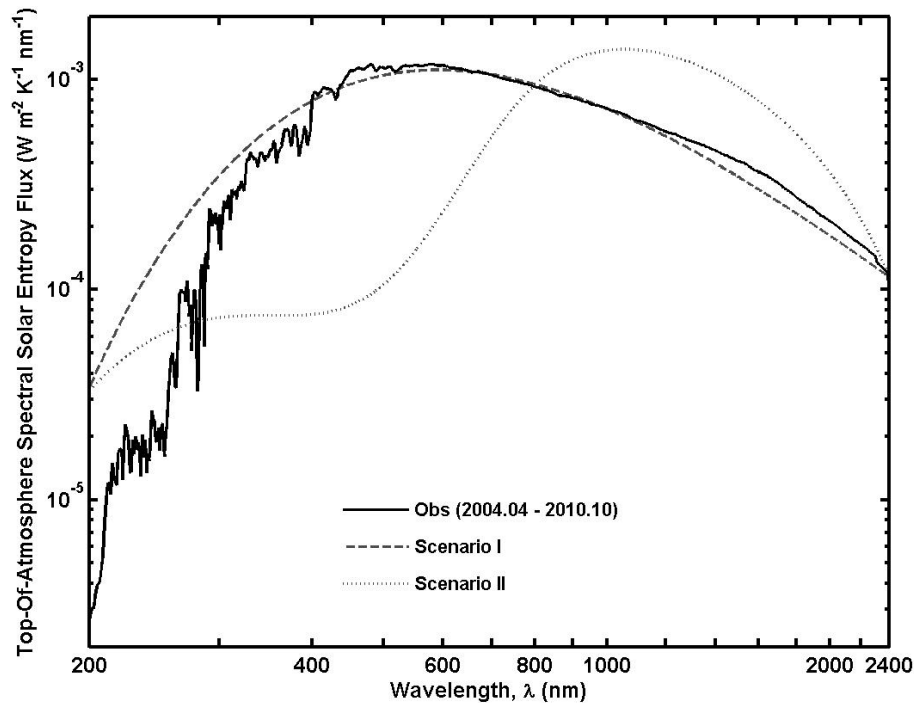


**Fig. 8.** The Earth's incident spectral solar radiation entropy flux for the three cases as shown in Figs. 6 or 7.

[Title Page](#)[Abstract](#)[Introduction](#)[Conclusions](#)[References](#)[Tables](#)[Figures](#)[◀](#)[▶](#)[◀](#)[▶](#)[Back](#)[Close](#)[Full Screen / Esc](#)[Printer-friendly Version](#)[Interactive Discussion](#)